

# Layer dependent band dispersion and correlations using tunable Soft X-ray ARPES

N. Kamakura<sup>1</sup>, Y. Takata<sup>1</sup>, T. Tokushima<sup>1</sup>, Y. Harada<sup>1</sup>, A. Chainani<sup>1,2</sup>, K. Kobayashi<sup>3</sup>, and S. Shin<sup>1,4</sup>

<sup>1</sup>RIKEN, Harima Institute, 1-1-1 Kouto, Mikazuki, Sayo, Hyogo 679-5148, Japan

<sup>2</sup> Institute for Plasma Research, Bhat, Gandhinagar 382 428, Gujarat, India

<sup>3</sup> SPring-8/JASRI Mikazuki, Hyogo 679-5198, Japan

<sup>4</sup>Institute for Solid State Physics, University of Tokyo, Kashiwanoha, Kashiwa, Chiba 277-8581, Japan

Soft X-ray Angle-Resolved Photoemission Spectroscopy is applied to study in-plane band dispersions of Nickel as a function of probing depth. Photon energies between  $h\nu = 190$  and 780 eV were used to effectively probe up to  $\sim 3\text{--}7$  layers ( $\sim 5\text{--}12$  Å). The results show layer dependent band dispersion of the  $\Delta_{2\downarrow}$  minority-spin band which crosses the Fermi level in 3 or more layers, in contrast to known top 1–2 layers dispersion obtained using ultra-violet rays. The layer dependence corresponds to an increased value of exchange splitting and reduced correlation effects in the bulk compared to the surface.

Angle-Resolved Photoemission Spectroscopy (ARPES) is a valuable tool to study the experimental band-structure(BS),  $w(\mathbf{k})$ , where  $w$  is energy and  $\mathbf{k}$  is momentum of electrons in a solid. Recent Ultra-violet-ARPES (ARUPS) studies of correlated materials have provided important results like spin and charge collective modes in a quasi 1-D (dimensional) metal [1], dimensional crossover [2], exotic characteristics of the high- $T_c$  cuprates [3], etc. While ARUPS is extremely well suited to study electronic BS of low-dimensional solids, it probes the top 1–2 layers of the surface [4]. In order to determine bulk BS of 3-D correlated systems which can depend on the probed layer [5, 6, 7, 8], it is meaningful to use higher energies. As the excitation energy is increased, the probing depth or mean free path(MFP) increases [9], but to date, no layer dependent variation of in-plane band dispersion (BD) beyond the top 2 layers has been reported. In this work, using tunable soft X-ray ARPES, we study layer dependence of in-plane BDs of Nickel metal.

Nickel is a prototype of a correlated ferromagnetic metal and has been extensively studied using PES and inverse-PES spectroscopies [10, 11, 12, 13, 14, 15, 16, 17, 18, 19]. Beginning with the work of Slater [20] and Stoner [21], the BS of Nickel has remained a suitable testing ground for a variety of experiments and theory. Recent theories have addressed the major inconsistencies with experiment. : The 3d bandwidth and exchange splitting(ES) of Nickel observed by ARUPS are reduced by 25% and 50%, respectively [10, 11, 12, 13, 14, 15], compared to the values obtained from spin-polarized local density approximation (s-LDA) calculations [22]. The 6 eV satellite obtained in PES experiments [16, 17, 18] is the two-hole bound state due to correlation effects. It is missing in BS calculations in the one-electron picture [22] but obtained in “generalized Hubbard models” [14, 19, 23] or the “LDA (GWA) + DMFT” (Dynamical Mean-Field Theory) [24, 25] which explicitly include Coulomb interactions. A recent study discusses the inability of s-LDA to reproduce the position of the minority spin state  $X_{2\downarrow}$  below  $E_F$  obtained by ARUPS [12, 14]. The energy position of  $X_{2\downarrow}$  states determines the elec-

tron count associated with the hole pocket of minority spin character at  $X$ -point, which influences the magnetic moment, a macroscopic property. Although recent theoretical efforts reproduce the experimental BS of Nickel by including correlation effects [14, 25], the results were compared with experimental BS obtained using ARUPS. The present study reports new experimental results of the bulk BS of Nickel obtained using soft X-ray ARPES.

Experiments were performed at beam line 27SU of SPring-8 [26] using linearly polarized light. ARPES was performed at 50 K with a total energy resolution of 50–160 meV. The beam line has a figure-8 undulator [27], enabling an easy switch of the polarization vector from horizontal(H)- to vertical(V)- polarization. Ni(100) surface was prepared by  $\text{Ar}^+$  sputtering and annealing. The surface was checked by core level photoemission spectra obtained using 780 eV photons and the contamination due to Oxygen and Carbon was measured to be  $< 1\%$ . The surface crystallinity was confirmed to be a sharp  $(1\times 1)$  LEED pattern.

ARPES measures  $w$  and  $\mathbf{k}$  of electrons in a solid according to the following equations [4].

$$\hbar\mathbf{k}_{\parallel} = \sqrt{2m(h\nu - w - \phi)} \sin \theta_e, \quad (1)$$

$$\hbar\mathbf{k}_{\perp} = \sqrt{2m\{(h\nu - w - \phi) \cos^2 \theta_e + V_0\}}, \quad (2)$$

where  $\mathbf{k}_{\parallel}$  and  $\mathbf{k}_{\perp}$  are parallel and perpendicular components of  $\mathbf{k}$ , respectively,  $\theta_e$  is electron emission angle,  $\phi$  is work function, and  $V_0$  is inner potential. The angular resolution of the electron energy analyzer was better than  $\pm 0.2^\circ$  which corresponds to resolutions of about  $\pm 0.014$ ,  $\pm 0.021$ , and  $\pm 0.028$  ( $2\pi/a_{Ni}$ ) in  $\mathbf{k}_{\parallel}$  at  $h\nu = 190$ , 435, and 780 eV, respectively (Eq. (1)). Eqs. (1) and (2) indicate that when ARPES with fixed  $h\nu$  is used for measurement of in-plane ( $\mathbf{k}_{\parallel}$ ) BDs,  $\mathbf{k}_{\perp}$  also changes. The variation of  $\mathbf{k}_{\perp}$  can be substantial in ARUPS [28], but diminishes with increasing  $h\nu$ , making it an advantage. In Fig. 1(a), we plot  $\mathbf{k}_{\perp}$  versus  $\mathbf{k}_{\parallel}$  in units of  $(2\pi/a_{Ni})$  for  $h\nu = 190$ , 435, and 780 eV in the experimental geometry of Fig. 1(b), using Eqs. (1) and (2) with  $V_0 = 9.3$  eV [29]. The spectra of  $\mathbf{k}_{\parallel} = 0$  at these  $h\nu$  are expected

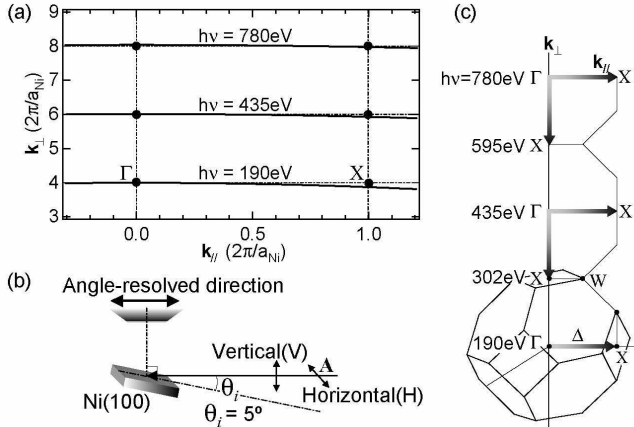


FIG. 1: (a)  $k_{\perp}$  versus  $k_{\parallel}$  for soft X-ray ARPES of Ni(100) for  $h\nu = 190, 435$  and  $780$  eV photons by the experimental geometry used(Fig. 1(b)). Fig. 1(c) shows the 3-D BZ of Ni(100) alongwith the probed sections.

to probe an equivalent  $k_{\perp}$  point ( $\Gamma$ ) in the 3-D Brillouin zone (BZ) of Ni(100)(Fig. 1(c)). We first validate this by  $h\nu$ - dependent ARPES in successive BZs (Figs. 2(a) and 2(b)). The changes in peak positions correspond to  $k_{\perp}$  BD, mainly due to  $\Delta_1$  band. The similarity of spectra in Figs. 2(a) and 2(b) measured in successive BZs confirm we are at equivalent momentum regions and the  $\Gamma$ -point can be precisely measured according to Eq. (2) even by soft X-ray ARPES. Further, since the difference of  $k_{\perp}$  along  $\Gamma$ - $X$  ( $\Delta$ -line) of  $k_{\parallel}$  is already small with 190 eV photons (Fig. 1(a)), the in-plane BD along  $\Gamma$ - $X$  can be measured by ARPES with 190, 435, and 780 eV photons. The probing depth or MFP is estimated to be about 5, 8, and 12 Å at  $h\nu = 190, 435$ , and  $780$  eV, respectively [9]. Thus we can probe up to the third, fifth, and seventh layer of equivalent regions in the 3-D BZ (Figs. 1(a)-(c)).

In Figs. 2(c) and 2(d) we show the ARPES spectra of Ni(100) excited by 780 eV photons with H- and V-polarization, from  $\Gamma$  to  $X$ . The spectra show angular dependence in  $\mathbf{k}$ -space from  $\Gamma$  to  $X$  due to BDs, as marked with triangles. At the  $\Gamma$ -point in Fig. 2(c), the two peaks correspond to the critical points  $\Gamma_{25'}$  and  $\Gamma_{12}$  at 1.21 eV and 0.51 eV binding energy. Two bands disperse from  $\Gamma_{25'}$  towards  $X$ -point and a third band disperses from  $\Gamma_{12}$ , corresponding to  $\Delta_2$ ,  $\Delta_5$ , and  $\Delta_2$  bands, respectively (Fig. 2(c)). Features due to a fourth weak band ( $\Delta_1$ ) are also barely seen. These BDs are almost consistent with ARUPS results [10, 11, 12, 13, 14, 15]. Especially, the energy positions at the high symmetry  $\Gamma$ - and  $X$ -point are very consistent with (spin-integrated) ARUPS results indicated by bars in Fig. 2(c). Fig. 2(d) (V-polarization) reproduces the energy positions of the critical points  $\Gamma_{12}$  and  $X_{5\uparrow}$ , with consistent BDs as in Fig. 2(c) (H-polarization), but enhances the  $\Delta_2$  band relative to other bands [30]. The results indicate that

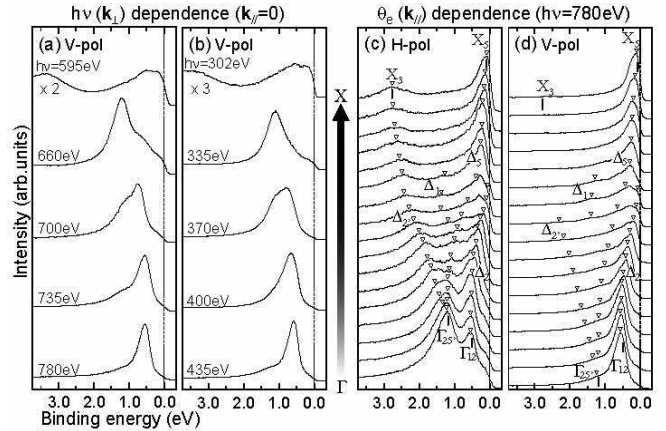


FIG. 2: For  $k_{\parallel} = 0$  and  $h\nu =$  (a)  $780$ – $595$  eV and (b)  $435$ – $302$  eV, nearly identical spectra in successive BZs, which are normalized by photon flux, verify the validity of the  $k_{\perp}$  points shown in Fig. 1. Soft X-ray ( $h\nu = 780$  eV) ARPES of Ni(100) along  $\Gamma$ - $X$  ( $\Delta$ -line) with (c) H and (d) V-polarization, where each spectrum is integrated over  $0.5^\circ$ . Peak positions ( $\nabla$ ) indicate BDs ( $\Delta_2$ ,  $\Delta_5$ ,  $\Delta_1$  and  $\Delta_{2'}$ ).

soft X-ray ARPES can be surely used to obtain BDs of solids. However, there is one important discrepancy in the present data compared with ARUPS results. The  $\Delta_2$  band crosses the  $E_F$  in the present spectra and its energy position at the  $X$ -point, that is  $X_2$ , is evidently above  $E_F$ . This is in contrast with ARUPS studies [10, 11, 12, 13, 14, 15] which show that the majority and minority bands of  $\Delta_2$  symmetry do not cross  $E_F$ , but remain below  $E_F$  all along the  $\Delta$ -line.

As a check of the  $\Delta_2$  BD measured using  $h\nu = 780$  eV, and if truly so, to investigate its deviation from ARUPS results, we measured BDs with  $h\nu = 435$  and  $190$  eV. In order to clearly see BDs, we plot band maps (BM) (second derivative of raw spectra after smoothing, e.g. Fig. 3(a) is a BM of spectra shown in Fig. 2(d)). Figs. 3(a)–(c) show BMs obtained with V-polarization using  $h\nu = 780$ ,  $435$ , and  $190$  eV, respectively. In Fig. 3(a), the  $\Delta_2$  BD can be followed unambiguously and the  $E_F$  crossing is clearly observed (arrow mark), corresponding to the  $\Delta_{2\downarrow}$  minority band. The  $\Delta_{2\uparrow}$  majority BD also can be seen in Fig. 3(a) but is more clear in Figs. 3(b) and 3(c), with  $X_{2\uparrow}$  located at 0.27 eV binding energy. The spectral intensity very close to the  $E_F$  crossing of  $\Delta_{2\downarrow}$  (Fig. 3(a), just next to the arrow mark), disperses to higher binding energy and is assigned to  $\Delta_{5\downarrow}$ . Additional confirmation comes from the  $435$  eV BM in Fig. 3(b) which shows nearly identical BDs, but for a small change of the  $E_F$  crossing point in  $\mathbf{k}$ -space (arrow mark). The changed BD of the  $\Delta_{2\downarrow}$  band with  $435$  eV photons (Fig. 3(b)) results in overlapping the  $\Delta_{5\downarrow}$  band at  $E_F$ , which are separated with  $780$  eV photons in Fig. 3(a). The most important result is obtained with the  $h\nu = 190$  eV BM shown in Fig. 3(c). This BM shows well-resolved majority ( $\Delta_{2\uparrow}$ ) and

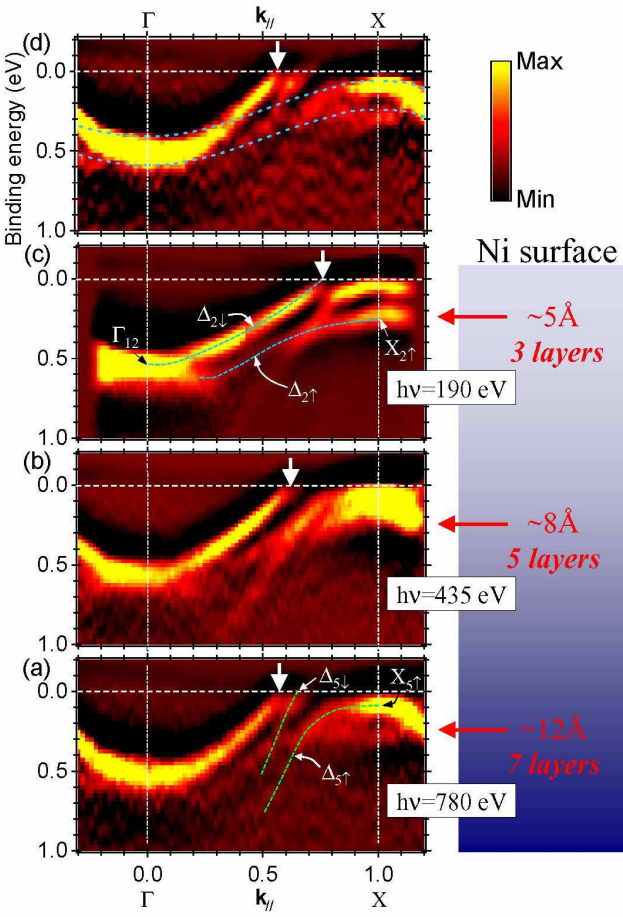


FIG. 3: Band maps of Ni(100) along  $\Gamma$ -X ( $\Delta$ -line) using (a)  $h\nu = 780$  eV, (b)  $435$  eV and (c)  $190$  eV, with V-polarization. Arrows indicate  $\mathbf{k}$ -points where the  $\Delta_{2\downarrow}$  band crosses  $E_F$ . Fig. 3(d) is obtained as  $I(780) - xI(435) - yI(190)$  with exponential factors  $x$  and  $y$  ( $I$ : intensity weighted by atomic cross-sections). The result is rather insensitive to the prefactors  $x$  and  $y$  as the changes are dominated by atomic cross-section effects. For Fig. 3(d),  $x = 0.6$ ,  $y = 0.33$ .

minority ( $\Delta_{2\downarrow}$ ) bands. Probing just beyond the ARUPS regime changes BDs which are clearly intermediate to the bulk BDs (obtained with  $h\nu = 435$  and  $780$  eV) and surface BDs obtained by ARUPS [10, 11, 12, 13, 14, 15]. The  $\Delta_{2\downarrow}$  band crosses  $E_F$  at  $0.57(\Gamma-X)$  in Fig. 3(a), at  $0.62(\Gamma-X)$  in Fig. 3(b), whereas it is  $0.76(\Gamma-X)$  in Fig. 3(c). Since the  $\Delta_{2\downarrow}$  BD changes systematically, the results indicate that the  $\Delta_2$  bandwidth and the ( $X_{2\uparrow} - X_{2\downarrow}$ ) ES is increased in the bulk compared to the ARUPS results. From ARUPS the ES is estimated to be  $170$  meV, an anomalously low ES measured only for the  $X_2$  point on the surface [12, 14, 19].

Since, at any photon energy, the experiments actually measure an integral of the intensity, weighted by an exponential factor for the MFP, we try to extract the bulk BD from ARPES with  $780$  eV photons. The ARPES with  $780$  eV photons is subtracted by a composite of  $435$  eV

and  $190$  eV spectra weighted by a roughly exponential factors and assuming atomic cross-sections. One such result is shown in Fig. 3(d) and confirms that the BD seen for bulk Ni are similar to the raw data of Fig. 3(a). In particular, the separate BDs are more clear at the  $X$  point. The data thus prove that the  $\Delta_{2\downarrow}$  BD is different in the bulk compared to surface sensitive ARUPS studies (overlaid as dashed lines).

The layer dependent BD is coupled to the widening of the  $\Delta_2$  band width observed in ARPES using high  $h\nu$ , suggesting weaker electron-electron correlations in the bulk. Theoretical calculations which include Coulomb correlations show that  $X_{2\downarrow}$  is located below  $E_F$  [14, 19, 23, 24, 25] in contrast to s-LDA calculations [22] and the  $6$  eV satellite is also reproduced [23, 24, 25]. Hence, we checked for variations of ARPES spectra in the  $6$  eV satellite region as a function of  $h\nu$  (Figs. 4(a) and 4(b)). The ARPES spectra show the  $\Delta_1$  band dispersing across and overlapping the  $6$  eV satellite between  $\Gamma$  to  $X$ , as expected from s-LDA calculations [22] and ARUPS studies [10, 11, 12, 13, 14, 15]. Even though the  $4sp$  character  $\Delta_1$  band crossing makes quantification very difficult, an attempt to do so with the  $\Gamma$  point spectra (Fig. 4(c)), where the  $\Delta_1$  band is separated, shows a reduction of  $\sim 20 \pm 4\%$  in the  $6$  eV satellite intensity on increasing  $h\nu$  from  $190$  to  $780$  eV. This confirms reduced correlations in the bulk [16, 17, 18, 23], which is consistent with the layer dependent change of  $\Delta_{2\downarrow}$  band dispersion in Fig. 3. Also, since the electron correlation in Nickel leads to a reduced ES compared to s-LDA calculation [19, 25], the reduced correlation is consistent

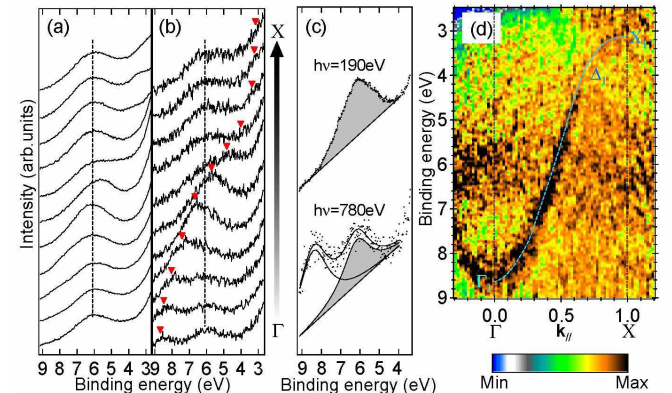


FIG. 4: ARPES spectra with  $h\nu =$  (a)  $190$  and (b)  $780$  eV, for the  $6$  eV satellite from  $\Gamma$  to  $X$ , normalized for area under the curve of the entire valence band. Triangles in (b) indicate  $\Delta_1$  BD obtained from Fig. 4(d). (c) A blow-up of  $6$  eV satellite feature at  $\Gamma$ -point for the same normalization. Curve fits (solid curves) indicate a reduction of  $\sim 20 \pm 4\%$  in  $6$  eV satellite intensity for  $h\nu = 780$  eV (shaded area), but no weakening of the correlation energy, consistent with its localized nature. (d) The BM between  $2.5$  and  $9.0$  eV binding energy showing  $\Delta_1$  BD (broken curve).

with the enhancement of ES observed at  $X_2$ . Since the 6 eV satellite feature is still observed with 780 eV photons as in angle-integrated X-PES studies [16], it shows that ARPES is necessary to check for the bulk to surface changes in the valence BS. In Fig. 4(d), we plot a BM for 2.5 to 9.0 eV binding energy and  $h\nu = 780$  eV, where  $\Delta_1$  BD is clearly seen, consistent with ARUPS results. We have also confirmed that the  $\Delta_1$  BD is similar to that obtained by applying the sum rule as discussed in Ref. [31].

Another important point to note is that the  $\Delta_5$  and  $\Delta_{2'}$  (Fig. 2(c)) BDs do not change with  $h\nu$  i.e. as a function of probing depth. Since  $\Delta_5$  and  $\Delta_{2'}$  band originate in  $t_{2g}$ -type states, it is not modified by electron correlations like the  $e_g$ -derived states [23]. Even between the  $e_g$ -derived states, the  $\Delta_2$  band ( $d_{x^2-y^2}$ ) possibly shows more layer dependent correlation than the  $\Delta_1$  band ( $d_{z^2-r^2}$ ) since the ( $d_{x^2-y^2}$ ) orbital extends outwards along the surface normal direction (100). This is similar to recent results showing varying correlations between the  $t_{2g}$ -orbitals of ( $d_{xy}$ ), ( $d_{xz}$ ), and ( $d_{yz}$ ) symmetry [5].

In conclusion, tunable soft X-ray polarization dependent ARPES makes it possible to resolve the changes in BDs with specified symmetry and layers. We observe layer dependent  $\Delta_{2\downarrow}$  band dispersion, which leads to an additional minority spin  $X_{2\downarrow}$  hole pocket. However, the  $\Delta_5$  and  $\Delta_{2'}$  ( $t_{2g}$ )-symmetry bands are not affected by the existence of the surface. The results show consistency of BD changes, correlation effects and ES being coupled to changes in the probing depth and the importance of Coulomb correlations in theoretical calculations for the surface electronic BS. Soft X-ray ARPES is thus shown to be a very important tool to study layer dependent BD of 3-D solids.

We thank Drs. H. Ohashi, Y. Tamenori, T. Ito, and P. A. Rayjada for help with experiments and Profs. A. Fujimori, T. Yokoya, A. Kotani, M. Taguchi, M. Usuda, T. Jo, and Dr. K. Horiba for valuable discussions.

Lett. **80**, 2885 (1998).; S.-K. Mo *et al.*, Phys. Rev. Lett. **90**, 186403 (2003).

- [9] S. Tanuma, C. J. Powell, and D.R. Penn, Surf. Interface anal., **11**, 57 (1988).
- [10] F. J. Himpsel, J. A. Knapp, and D. E. Eastman, Phys. Rev. B **19**, 2919 (1979).
- [11] W. Eberhardt, and E. W. Plummer, Phys. Rev. B **21**, 3245 (1980).
- [12] P. Heimann, F. J. Himpsel, and D. E. Eastman, Solid State Commun. **39**, 219 (1981).
- [13] H. Mårtensson and P. O. Nilsson, Phys. Rev. B **30**, 3047 (1984).
- [14] J. Bünenmann *et al.*, Europhys. Lett. **61**, 667 (2003).
- [15] A. Kakizaki *et al.*, Phys. Rev. Lett. **72**, 2781 (1994).; T. Greber, T. J. Kreutz, and J. Osterwalder, Phys. Rev. Lett. **79**, 4465 (1997).
- [16] S. Hüfner *et al.*, Solid State Commun. **11**, 323 (1972).
- [17] C. Guillot, *et al.*, Phys. Rev. Lett. **39**, 1632 (1977).
- [18] T. Kinoshita *et al.*, Phys. Rev. B **47**, 6787 (1993).; B. Sinkovic *et al.*, Phys. Rev. Lett. **79**, 3510 (1997).
- [19] M. Donath, Surf. Sci. Rep. **20**, 251 (1994).
- [20] J. C. Slater, Phys. Rev. **49**, 537 (1936).
- [21] E. C. Stoner, Proc. Roy. Soc. A **165**, 372 (1938).
- [22] C. S. Wang, and J. Callaway, Phys. Rev. B **15**, 298 (1977).
- [23] A. Liebsch, Phys. Rev. Lett. **43**, 1431 (1979).
- [24] A. I. Lichtenstein, M. I. Katsnelson, and G. Kotliar, Phys. Rev. Lett. **87**, 067205 (2001).
- [25] S. Biermann, F. Aryasetiawan, and A. Georges, Phys. Rev. Lett. **90**, 086402 (2003).
- [26] H. Ohashi *et al.*, Nucl. Instrum. Meth. A **467-468**, 529 (2001).
- [27] T. Tanaka, and H. Kitamura, J. Synchrotron Radiation **3**, 47 (1996).
- [28] It is also possible to measure  $\mathbf{k}_{\parallel}$  band dispersions in the constant final state (CFS) mode without  $\mathbf{k}_{\perp}$  variation compared to the energy distribution curve (EDC) mode described, even with ARUPS, see e.g. *Photoemission in Solids*, edited by M. Cardona and L. Ley (Springer-Verlag, Berlin, 1978), Vol. I, Chap. 6, p. 261.
- [29] Since our experimental geometry is near grazing incidence, the momentum transfer of the photon results in a constant shift of parallel component of the momentum  $\mathbf{k}_{\parallel}$ , while  $\mathbf{k}_{\perp}$  is negligibly influenced. This is understood from the measured spectra which show constant shifts in  $\mathbf{k}_{\parallel}$  by  $0.22(\Gamma - X)$ , while the  $\mathbf{k}_{\perp}$  negligibly shifts, for 780 eV. The shift of  $\mathbf{k}$  is identified from accurate determination of the high symmetry points  $\Gamma$  and  $X$ .
- [30] In Fig. 2 (a) and (b),  $\Delta_1$  band should be mainly observed due to dipole selection rules and the intensity decrease at  $X$ -point seen in the figure is caused by the  $\Delta_1$  band moving above  $E_F$ , as also expected from ARUPS. In Fig. 2(c) and (d), on the other hand, bands with all symmetries along  $\Delta$  can be observed because of the measurement of the in-plane band dispersion, and the relative intensity of each band is governed by matrix elements. In addition, the differences in spectra is also attributed to the different volumes sampled with the different photon energies used.
- [31] H. J. Freund *et al.*, Phys. Rev. Lett. **50**, 768 (1983).

---

- [1] P. Segovia *et al.*, Nature **402**, 504 (1999).
- [2] T. Valla *et al.*, Nature **417**, 627 (2002).
- [3] A. Lanzara *et al.*, Nature **412**, 510 (2001).; A. Kaminski *et al.*, Nature **416**, 610 (2002).; Z. M. Yusof *et al.*, Phys. Rev. Lett. **88**, 167006 (2002).
- [4] E. W. Plummer and W. Eberhardt, Adv. Chem. Phys. **49**, 533 (1982).
- [5] A. Liebsch, Phys. Rev. Lett. **90**, 096401 (2003).; S. Schwieger, M. Potthoff, and W. Nolting, Phys. Rev. B **67**, 165408 (2003).
- [6] O. Rader *et al.*, Europhys. Lett. **39**, 429 (1997).
- [7] A. Sekiyama *et al.*, Nature **403**, 396 (2000).
- [8] K. Maiti, P. Mahadevan, and D. D. Sarma, Phys. Rev.